

# Smoothed Molecular Dynamics for Large Step Time Integration

Yan Liu<sup>1</sup>, Xiong Zhang<sup>1</sup>, K. Y. Sze<sup>2</sup> and Min Wang<sup>1</sup>

**Abstract:** In molecular simulations, the frequencies of the low-frequency modes are many orders of magnitude lower than those of the high-frequency modes. Compared with the amplitudes of the low-frequency modes, the amplitudes of the high-frequency modes are often negligible and, thus, least interesting. As dictated by the period of the highest frequency mode, the critical time step for stable time integration can be significantly increased by suppressing the negligible high-frequency modes yet the solution remains virtually intact. In this light, a smoothed molecular dynamics (SMD) approach is proposed to eliminate the high-frequency modes from the dynamical system through the use of a regular background grid. By manipulating the grid size, it is possible to increase the critical time step significantly with respect to that of the conventional molecular dynamics (MD). The implementation of SMD is very similar to the conventional MD. Any time integrators and inter-atomic potentials used in the conventional MD can be equally adopted in SMD. The coupling of MD and SMD methods is briefly investigated, and the similarity between MD and SMD methods enables a simple and concise coupling. Examples on 1D atom chains and 3D tension/compression of single crystal show that the proposed SMD method and the conventional MD method yield close results yet the time step of the former can be one order higher than that of the latter. Tension of a cracked single crystal is examined to verify the coupling method, and the yield point can be captured precisely by the coupling method.

**Keyword:** Molecular dynamics, Critical time

step, Material point method, Background grid.

## 1 Introduction

In molecular dynamics (MD) simulations, the Newtonian equations of motion

$$m_i \ddot{\mathbf{r}}_i = \mathbf{F}_i(\mathbf{r}) \equiv -\frac{\partial E(\mathbf{r})}{\partial \mathbf{r}_i} \quad (1)$$

are solved numerically to obtain the distribution of the atoms in a molecular system [Allen and Tildesley (1989)]. In Eq. (1),  $\mathbf{r}_i$  and  $m_i$  are respectively the position vector and the mass of atom  $i$ . Moreover,  $\mathbf{F}_i$  is the force vector acting on the atom,  $\mathbf{r}$  is the vector that contains the positions of all atoms and  $E$  is the empirical potential energy function of the system.

A typical integrator used in MD is the leap-frog/Verlet method [Verlet (1967)] which can be expressed as

$$\mathbf{p}_i^{n+1/2} = \mathbf{p}_i^n + \frac{\Delta t}{2} \mathbf{F}_i(\mathbf{r}^n) \quad (2)$$

$$\mathbf{r}_i^{n+1} = \mathbf{r}_i^n + \Delta t \mathbf{p}_i^{n+1/2} / m_i \quad (3)$$

$$\mathbf{p}_i^{n+1} = \mathbf{p}_i^{n+1/2} + \frac{\Delta t}{2} \mathbf{F}_i(\mathbf{r}^{n+1}) \quad (4)$$

where  $\mathbf{p}_i = m_i \dot{\mathbf{r}}_i$  is the momentum of atom  $i$  and a quantity affixed with superscript  $n$  refers to its solution at time  $n\Delta t$ .

Computation of the forces acting on the atoms involves evaluating and summing all the inter-atomic forces acting in the system. It is expensive and should be conducted as infrequently as possible. Unfortunately, the time step  $\Delta t$  cannot exceed some limit value, otherwise the time integration will be numerically unstable. The limit of the time step  $\Delta t$  is defined as the critical time step. In MD, the oscillation periods of the high-frequency modes are many orders of magnitude smaller than

<sup>1</sup> Department of Engineering Mechanics, Tsinghua University, Beijing 100084, P. R. China

<sup>2</sup> Department of Mechanical Engineering, The University of Hong Kong, Hong Kong SAR, P. R. China

those of the low-frequency modes whose amplitudes are dominating and, thus, constituting the real concern [Schlick, Skeel, Brunger, Kale, Board Jr., Hermans, and Schulten (1999)]. From classical linear stability analysis, the critical time step for the Verlet method is  $\varepsilon/\pi$  where  $\varepsilon$  is the period of the highest frequency mode [Verlet (1967)]. The nonlinear stability analysis leads to the value to  $\varepsilon/(\sqrt{2}\pi)$  [Schlick, Mandziuk, Skeel, and Srinivas (1998)]. Consequently, the typical stable time step used in molecular simulation is in the order of femtosecond. This time scale leads to huge computing load and imposes severe limitation on the applicability of MD to real world problems. Various methods have been suggested to alleviate the restriction on the time step. Among these are the constrained dynamics, multiple-time-stepping method, implicit methods, multibody dynamics and subspace method.

Generally speaking, force fields in molecular dynamics for macromolecules can be classified to bond stretching, bond bending and torsion, short-range non-bonded forces and long-range non-bonded forces [Humphreys, Friesner, and Berne (1994)]. Non-bonded forces vary much slower than bonded forces. The highest frequency modes are due to bond deformation. Larger time step is possible by imposing constraints for removing these modes [Leimkuhler and Reich (1994); Reich (1995)]. The practice leads to a set of constrained equations of motion which can be discretized by the SHAKE/RATTLE method [Andersen (1983); Ryckaert, Ciccotti, and Berendsen (1977)]. Reich also suggested a constrained formulation that maintains the flexibility of the system while, at the same time, suppresses the high-frequency components in the solutions and thus enables a larger time step [Reich (1995)]. The method employs a mean force field which is yielded by an averaging process over the fastest degrees of motion.

The idea of multiple-time-stepping (MTS) is to evaluate different force terms by using different time steps. A typical MTS integrator is the RESPA multiple-time-stepping impulse method [Grubmuller, Heller, Windemuth, and et al (1991); Tuckerman, Berne, and Martyna

(1992)]. In this method, the force is split into fast and slow components, and Trotter factorization of the Liouville propagator is adopted [Humphreys, Friesner, and Berne (1994)]. The inexpensive fast interactions are updated more frequently while the costly slow forces are updated less frequently. RESPA is designed for large biomolecular system, but it is also ready for other systems. RESPA was applied in *ab initio*/quantum molecular dynamics [Gibson and Carter (1993); Reich (1999)], in combination with Ewald and particle mesh Ewald method [Zhou, Harder, Xu, and Berne (2001)], and simulation of dislocation and grain boundaries [Li and Yang (2005)]. Limitations on the step size in MTS integrators are still severe and these are mostly due to stability rather than accuracy [Izaguirre, Ma, Matthey, Willcock, Slabach, Moore, and Viamontes (2002)]. The limitation comes mainly from nonlinear resonances [Ma, Izaguirre, and Skeel (2003)]. Izaguirre, Reich, and Skeel (1999) and Izaguirre, Catarello, Wozniak, and Skeel (2001) proposed Langevin dynamics or mollified scheme to stabilize RESPA method. The Langevin-Implicit/Normal mode scheme (LIN) [Zhang and Schlick (1993, 1994)] is another multiple-time-stepping method. It resolves the fast motion by linearizing the equations of motion and obtains the residual motion by implicit integration. LIN permits comparatively longer time steps. As the computational expense for each time step is rather high, LIN yields only modest overall efficiency gain.

Various researchers have studied the use of implicit/semi-implicit methods with the hope of circumventing the stability restriction and enabling larger time steps. A popular implicit discretization is the (implicit) midpoint method [Hairer and Wanner (1991); Ascher and Reich (1998, 2000)]. Since fully implicit methods are very expensive when long-range forces are present, semi-implicit methods [Reich (1996)] are also proposed. In these methods, the force is split into weak forces and strong forces. Only the highly oscillatory components which are caused by the strong forces are integrated by an implicit method.

Different from separation of different types of

forces in the above methods, subspace method uses cut-off in frequency domain. Dey, Rabitz, and Askar (2003) proposed an optimal reduced method to find optimal degrees of freedom and the cut-off frequency to achieve a minimum cost functions.

The interaction of molecules are very similar to those of multibody system. MBO(N)D [Chun, Padilla, Chin, M, Karlov, Alper, Soosaar, Blair, Becker, Caves, Nagle, Haney, and Farmer (2000)] is an order  $N$  multibody method, which grouped atoms into flexible and/or rigid bodies. The forces between molecules are simulated with hinges and elastic springs. In this manner, the dominated low-frequency motion of molecules can be treated efficiently.

Review of approaches to enlarge time step of molecular dynamics can be found in literature [Schlick, Skeel, Brunger, Kale, Board Jr., Hermans, and Schulten (1999)]. Constrained methods are easy to implement, but they are sometimes too coarse to describe the motion. The idea of MTS methods is natural and intriguing, but MTS methods are mainly limited by stabilization. The time step of MTS methods cannot be increased too much, which hinders their broader application. Implicit methods, subspace method and multibody dynamics may obtain longer time step. A common drawback of the three kinds of methods is that they require nontrivial computational cost in addition to time integration. To sum up, the kernel spirit to enlarge time step is to find an appropriate way to deal with high-frequency motions and reserve major results of the low-frequency motion.

The numerical stability is limited by the presence of the high-frequency modes. Under most circumstances, the high-frequency modes possess negligible amplitudes and practical interest. Hence, these small and fast oscillations can be filtered out to arrive at a new system which mainly describes the slow but large dynamic components of the original system. In such a way, the time step can be increased significantly. In fact, numerical stability issue similar to that of MD also exists in other dynamic problems. A distinct example is the hyper-velocity impact prob-

lem in which the explicit Lagrangian finite element method is commonly used. Due to element distortion and mesh entanglement, the critical time step decreases considerably as the impact process proceeds. The computational cost per unit time in simulating the process may be increased to an unacceptable level. Among the various approaches for hyper-velocity impact simulation, the Material Point Method (MPM) [Sulsky, Chen, and Schreyer (1994); Zhang, Sze, and Ma (2006)] which discretizes the material with a collection of particles or material points is computationally efficient. In each time step, the particles are attached to a regular background grid and they deform with the grid. The momentum equations are solved on the grid points instead of particles. Consequently, the critical time step is controlled by the grid size rather than the inter-particle spacing. At the end of each time step, the deformed grid is discarded and a new regular background grid is used for the next time step. Usually, the same regular grid is used for all time steps, hence the grid size and thus the critical time step would remain constant during the impact process.

In this paper, a smoothed molecular dynamics (SMD) approach is proposed by introducing the computational strategy of MPM into molecular simulations. The high-frequency oscillation modes are eliminated from the dynamic system via the use of a regular background grid. The critical time step can be increased significantly and by as much as one order compared with that of the conventional MD.

## 2 Smoothing the Motion of Atoms

Reich suggested a mean force field approach [Reich (1995)] in which the force field is obtained by an averaging process over the fastest degrees of motion and the high-frequency components can be eliminated. The high-frequency components can also be eliminated by attaching the atoms to the grid cells which are defined by a regular background grid at the beginning of each time step, see Fig. 1.

Let  $\mathcal{C}_I$  be the set of adjacent grid cells connected to grid point  $I$ ,  $\mathcal{P}_I$  be the set of grid points that define all the grid cells in  $\mathcal{C}_I$  and  $\mathcal{A}_I$  be the set of

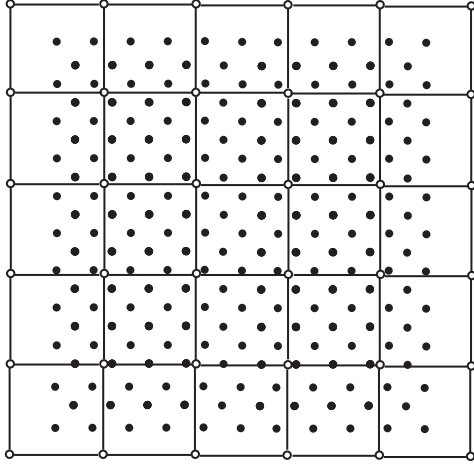


Figure 1: Motion of atoms are smoothed by attaching the atoms rigidly to the background grid in every time step

atoms within  $\mathcal{C}_I$ . In this paper, the lowercase subscript indices ( $i, j$ ) refer to atoms and the uppercase ones ( $I, J$ ) refer to grid points. Hexahedral grid cell defined by eight grid points is adopted.

Because the atoms are attached to the grid cells, the value of the unknown variable  $f$  for atom  $i$  can be obtained from the values of  $f$  at the grid points by using typical finite element approximation as

$$f_i = \sum_{J \in \mathcal{P}_I} N_{Ji} f_J \quad \forall i \in \mathcal{A}_I \quad (5)$$

When grid point  $J$  defines the grid cell that embraces atom  $i$ ,  $N_{Ji} = N_J(\mathbf{r}_i)$  is the finite element shape function associated with grid point  $J$  evaluated at atom site  $\mathbf{r}_i$ . Otherwise,  $N_{Ji}$  is zero.  $N_J(\mathbf{x})$  varies for different types of element. For 3D 8-node cuboid element,  $N_J(\mathbf{x})$  is given by the following trilinear interpolation

$$N_J = \frac{1}{8}(1 + \xi \xi_J)(1 + \eta \eta_J)(1 + \zeta \zeta_J) \quad (6)$$

where  $\xi$ ,  $\eta$  and  $\zeta$  are the local coordinates, which take on their nodal values  $(\xi_J, \eta_J, \zeta_J)$  of  $(\pm 1, \pm 1, \pm 1)$  at the grid points.

Similar to Eq. (5), the velocity and the accelera-

tion of an atom  $i$  can be obtained by

$$\dot{\mathbf{r}}_i = \sum_{J \in \mathcal{P}_I} N_{Ji} \dot{\mathbf{r}}_J, \quad \forall i \in \mathcal{A}_I \quad (7)$$

$$\ddot{\mathbf{r}}_i = \sum_{J \in \mathcal{P}_I} N_{Ji} \ddot{\mathbf{r}}_J, \quad \forall i \in \mathcal{A}_I \quad (8)$$

In the proposed method, the high-frequency oscillation components are eliminated from the motion of atoms by attaching the atoms to the background grid using which the motion of atoms are smoothed. Therefore, the proposed method is termed as smoothed molecular dynamics (SMD). Unlike the conventional MD, the spatial resolution of SMD is controllable. To enable a larger allowable time step, a larger grid cell size is required at the expense of the accuracy in the spatial discretization.

However, the grid cell will be distorted and entangled if the material experiences severe deformation. This will reduce the critical time step significantly. To avoid this difficulty, the deformed grid is discarded at the end of each time step and a new regular grid is used in the next time step. It is generally adequate to use the same regular grid in all time steps. The background grid is therefore essentially fixed in the space. In this way, the critical time step which depends on the grid cell size can be kept constant.

### 3 Time Integration

In the proposed SMD, the atoms do not move independently as in the conventional MD. The velocity and acceleration of atoms depend on their grid point values via Eqs. (7) and (8). Instead of solving the equations of motion for the atoms, those for the grid points are solved. The equation of motion of grid point  $I$  can be established by mapping the equations of motion (Eq. (1)) of all atoms

$$\sum_{i \in \mathcal{A}_I} N_{Ii} m_i \ddot{\mathbf{r}}_i = \mathbf{F}_I \quad (9)$$

in which

$$\mathbf{F}_I = \sum_{i \in \mathcal{A}_I} N_{Ii} \mathbf{F}_i(\mathbf{r}) \quad (10)$$

is the grid point force. Substituting Eq. (8) into Eq. (9) leads to

$$\sum_{J \in \mathcal{P}_I} M_{IJ} \ddot{\mathbf{r}}_J = \mathbf{F}_I \quad (11)$$

where

$$M_{IJ} = \sum_{i \in \mathcal{A}_I} m_i N_{Ii} N_{Ji} \quad (12)$$

It is noted that the above mass matrix  $\mathbf{M}$  is banded but not diagonal. Using a non-diagonal mass matrix will increase the computational cost significantly because solving linear algebraic equations simultaneously are required to obtain  $\ddot{\mathbf{r}}_J$ . The lumped mass approach, which is very popular in the finite element method, is used in SMD to save the computational time. The lumped mass approach replaces the diagonal element of mass matrix with the summation of all the elements in the same row, and set all the other non-diagonal elements zero. Owing to the lumped mass approach, Eq. (11) can be further simplified to

$$M_I \ddot{\mathbf{r}}_I = \mathbf{F}_I \quad (13)$$

where

$$M_I = \sum_{J \in \mathcal{P}_I} M_{IJ} = \sum_{J \in \mathcal{P}_I} \sum_{i \in \mathcal{A}_I} m_i N_{Ii} N_{Ji} = \sum_{i \in \mathcal{A}_I} m_i N_{Ii} \quad (14)$$

after invoking the relationship  $\sum_J N_J(\mathbf{x}) = 1$  for arbitrary field point  $\mathbf{x}$ . Eq. (13) is much easier to solve than Eq. (11) because no matrix inversion is involved.

Mapping from atoms to grid points conserves the total forces, the total linear momenta and the total angular momenta of the system. For example, the total linear momenta of the grid points

$$\sum_I \mathbf{p}_I = \sum_I \sum_{j \in \mathcal{A}_I} N_{Ij} \mathbf{p}_j = \sum_{j \in \mathcal{A}_I} \left( \sum_I N_{Ij} \right) \mathbf{p}_j = \sum_{j \in \mathcal{A}_I} \mathbf{p}_j \quad (15)$$

which is exactly that of the atoms. The formula  $\sum_I N_I(\mathbf{r}_j) = 1$  is also used in Eq.(15). The conservation of angular momenta can be derived in the

same way

$$\begin{aligned} \sum_I \mathbf{r}_I \times \mathbf{p}_I &= \sum_I \mathbf{r}_I \times \sum_{j \in \mathcal{A}_I} N_{Ij} \mathbf{p}_j \\ &= \sum_{j \in \mathcal{A}_I} \left( \sum_I N_{Ij} \mathbf{r}_I \right) \times \mathbf{p}_j \\ &= \sum_{j \in \mathcal{A}_I} \mathbf{r}_j \times \mathbf{p}_j \end{aligned} \quad (16)$$

It may be interesting to see what will happen when the grid cell size approaches zero. The acceleration of an atom  $i$  obtained in SMD method is given by

$$\begin{aligned} \ddot{\mathbf{r}}_i &= \sum_{J \in \mathcal{P}_I} N_{Ji} \ddot{\mathbf{r}}_J = \sum_{J \in \mathcal{P}_I} N_{Ji} \frac{\mathbf{F}_J}{M_J} \\ &= \sum_{J \in \mathcal{P}_I} \frac{N_{Ji}}{\sum_{j \in \mathcal{A}_I} m_j N_{Jj}} \left( \sum_{k \in \mathcal{A}_I} N_{Jk} \mathbf{F}_k \right), \forall i \in \mathcal{A}_I \end{aligned} \quad (17)$$

When the grid cell size decreased to a certain level, any arbitrary pair of atoms do not contribute to the equations of motion of the same background grid point. Consequently, the summations over  $j$  and  $k$  in Eq. (17) will be degenerated to single value of  $i$ , which leads to

$$\ddot{\mathbf{r}}_i = \sum_{J \in \mathcal{P}_I} \frac{N_{Ji}}{m_i N_{Ji}} N_{Ji} \mathbf{F}_i = \left( \sum_{J \in \mathcal{P}_I} N_{Ji} \right) \frac{\mathbf{F}_i}{m_i} = \frac{\mathbf{F}_i}{m_i}, \quad \forall i \in \mathcal{A}_I \quad (18)$$

which is identical to the acceleration calculated by conventional MD.

Any time integration scheme used in the conventional MD can be used in SMD to solve Eq. (13). Taking the velocity Verlet scheme as an example, the typical SMD time step starting at time  $n\Delta t$  where  $\Delta t$  is the time step is outlined as follows.

1. Establish a new regular grid. However, if the regular grid established at time  $(n-1)\Delta t$  still cover all the atoms at time  $n\Delta t$ , it can be used and a new regular grid is not needed.

2. Calculate the grid point mass

$$M_I^n = \sum_{i \in \mathcal{A}_I} m_i N_{Ii}^n, \quad (19)$$

the grid point force

$$\mathbf{F}_I^n = \sum_{i \in \mathcal{A}_I} N_{II}^n \mathbf{F}_i(\mathbf{r}^n), \quad (20)$$

and the nodal momentum

$$\mathbf{p}_I^n = \sum_{i \in \mathcal{A}_I} N_{II}^n m_i \dot{\mathbf{r}}_i^n \quad (21)$$

at time  $n\Delta t$ . In Eq. (20),  $\mathbf{F}_i(\mathbf{r}^n) = -\partial E(\mathbf{r}^n)/\partial \mathbf{r}_i$  is the inter-atomic force at time  $n\Delta t$ .

3. Calculate the nodal momentum and atom velocity at the intermediate time  $(n+1/2)\Delta t$  as

$$\mathbf{p}_I^{n+1/2} = \mathbf{p}_I^n + \frac{\Delta t}{2} \mathbf{F}_I^n \quad (22)$$

$$\dot{\mathbf{r}}_i^{n+1/2} = \dot{\mathbf{r}}_i^n + \frac{\Delta t}{2} \sum_{I \in \mathcal{P}_I} N_{II}^n \mathbf{F}_I^n / M_I^n \quad (23)$$

4. Update the atom position

$$\mathbf{r}_i^{n+1} = \mathbf{r}_i^n + \Delta t \sum_{I \in \mathcal{P}_I} N_{II}^n \mathbf{p}_I^{n+1/2} / M_I^n \quad (24)$$

and the grid point force

$$\mathbf{F}_I^{n+1} = \sum_{i \in \mathcal{A}_I} N_{II}^n \mathbf{F}_i(\mathbf{r}^{n+1}) \quad (25)$$

at time  $(n+1)\Delta t$ .

5. Update the atom velocity at time  $(n+1)\Delta t$

$$\dot{\mathbf{r}}_i^{n+1} = \dot{\mathbf{r}}_i^{n+1/2} + \frac{\Delta t}{2} \sum_{I \in \mathcal{P}_I} N_{II}^n \mathbf{F}_I^{n+1} / M_I^n \quad (26)$$

6. Discard the deformed background grid.

It should be noted that the atom positions and velocities are updated by using the interpolated grid point velocities and accelerations, respectively, instead of being updated directly by atomic velocities and accelerations. Updating by increments can avoid possible numerical damping, as pointed out by the research of MPM method [Bardhagen and Kober (2004)].

#### 4 Combination of MD and SMD

As discussed in the previous sections, enlarging time step in SMD method is mainly based on filtering out high-frequency motion that cannot be represented by the mesh. Filtering high-frequency motion is not essential to the results of many atomic and molecular systems. In some situations, however, rearrangements or discontinuities of the atomic lattices (e.g. dislocation, crack, bond breakage, bond formation, etc.) occur, it is desirable to use the atomic resolution in some localized regions to capture the interesting high-frequency motion generated by the discontinuities, while to use SMD in the other region to save the computational cost. The idea of region division has been adopted in some popular combined atomic and continuum literatures, where the localized region is simulated by MD approach, while the rest far-field region is represented by continuum computational approaches such as finite element methods or meshfree methods [Tan and Yang (1994); Broughton, Abraham, Bernstein, and Kaxiras (1999); Wagner and Liu (2003); Shen and Atluri (2004, 2005); Lu, Daphalapurkar, Wang, Roy, and Komanduri (2006)]. Generally speaking, the continuum region is a coarse representation of the problem so that great computational resources may be saved by the combined approach. This kind of approach is always called concurrent multiscale coupling. The realization of concurrent coupling is not trivial though the idea is natural. For example, in some popular concurrent multiscale coupling methods, a transition zone must be introduced to achieve seamless coupling. The element size or nodal spacing of the continuum should be decreased to the lattice constant.

The coupling of MD and SMD is portrayed in Fig. 2, it is assumed that some discontinuities happen in the central region. MD is adopted in the central region, and SMD is used elsewhere. From the flowcharts of MD and SMD methods, it can be seen that SMD is very similar to MD except that the velocity or acceleration is smoothed by mapping process. Only a criterion is needed to justify what region an atom resides in. If an atom is in the MD region, it follows the flowchart of MD; other-

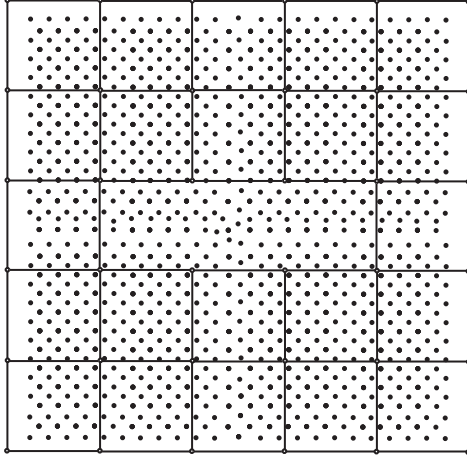


Figure 2: Coupling between MD and SMD

wise it follows that of SMD. No special treatment is needed for the interface of MD and SMD regions. Interactions between the two regions will be included naturally by the interactive forces between atoms in different regions. The critical time step for the two regions are not consistent, and a multiple time scale algorithm can always be used for the coupling method. Another method to deal with the localized problem is to use hierarchical adaptive background grid in which the grid size shrinks to the atomic scale in the localized regions. This is also reasonable since it has been shown that SMD method will degenerate to MD method if the grid cell size is below some critical value.

A schematic illustration of multiple-time-step coupling of MD and SMD methods is shown in Fig. 3. Atom  $i$  belongs to MD region and atom  $i-1$  belongs to SMD region. A smaller time step  $\Delta t_A$  is assigned to MD region and a larger time step  $\Delta t_B$  to SMD region. Assume that  $\Delta t_B/\Delta t_A = m$ , where  $m$  is an integer. The symbol  $n+[k]$  represents the  $k$ -th substep between time steps  $n$  and  $n+1$ , and  $n+[m] = n+1$ . The calculation of acceleration of an atom needs the positions of its nearest neighbors. For example, calculating  $\ddot{r}_i$  needs the information of  $r_{i-1}$ ,  $r_i$  and  $r_{i+1}$  as shown in Fig. 3. The equations of motion of atoms  $1, 2, \dots, i-2$  and  $i+1, i+2, \dots$  can be integrated easily because these atoms do not interact with atoms in the other region. The integration of equa-

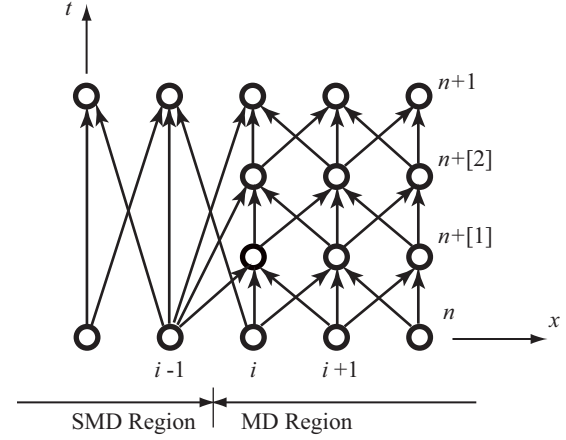


Figure 3: Multiple-time-step coupling of MD and SMD methods

tions of motion of atom  $i$ , however, requires some assumption due to lack of the position of atom  $i-1$  at substeps  $n+[1], n+[2], \dots, n+[m-1]$ .

Assumption of constant acceleration [Belytschko and Lu (1993)] is adopted in this paper, in which the accelerations of atoms interacting with atoms in MD region are assumed to be constant between time steps  $n$  and  $n+1$  and equaling to those at time step  $n$ . For the illustrated example in Fig. 3, the assumption is applied for atom  $i-1$  so that the pseudo-position and the pseudo-velocity at time step  $n+[j]$  can be given as follows

$$r_{i-1}^{n+[j]} = r_{i-1}^n + (j\Delta t_A) \dot{r}_{i-1}^n + \frac{1}{2} (j\Delta t_A)^2 \ddot{r}_{i-1}^n \quad (27)$$

$$\dot{r}_{i-1}^{n+[j]} = \dot{r}_{i-1}^n + (j\Delta t_A) \ddot{r}_{i-1}^n \quad (28)$$

The equations of motion of atom  $i$  can be integrated with the pseudo-position and the pseudo-velocity of atom  $i-1$ . The formulae are the same for more complicated and high dimensional cases except that more atoms near the interface of two regions are involved.

## 5 Numerical Examples

### 5.1 Impact of Two 1D Atom Chains

Impact of the two atom chains in Fig. 4 is firstly considered. Each chain contains 201 atoms. Adjacent atoms interact according to 1D harmonic

potential  $U_{ij} = 0.5k(|x_i - x_j| - h_0)^2$  where  $h_0$  is the equilibrium distance. The two chains are initially  $h_0$  apart and they move towards each other with an initial speed  $v = 0.1$ . The rightmost atom of the left chain and the leftmost atom of the right chain also interacts according to the 1D harmonic potential.

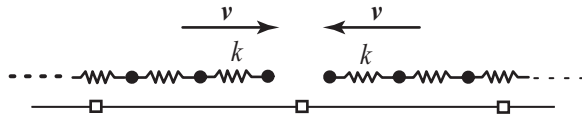


Figure 4: Impact of two atom chains. Dots denote atoms and squares denote grid points

The potential parameter  $k$ , the atom mass  $m$  and the equilibrium distance  $h_0$  are taken as the basic units and the units of other quantities are derived accordingly. For simplicity,  $k$ ,  $m$  and  $h_0$  are taken to be unity. All the variables are dimensionless in 1D examples. With the values, the critical MD time step size  $\Delta t^{cr}$  equals 1.0.

Numerous SMD simulations with the grid cell sizes  $\Delta x$  ranging from 2 to 40 and the time steps  $\Delta t$  ranging from 1 to 20 are attempted. The total energy is plotted against time in Fig. 5. As the system is conservative, the analytical total energy does not vary with time and is equal to 5. Three representative SMD results with  $(\Delta x, \Delta t)$  equal to (2, 1), (10, 8) and (40, 20) are included in Fig. 5. It can be seen that all results agree well with the MD results obtained by using  $\Delta t = 0.5$ . The loss of total energy in SMD,  $E_l$ , does not exceed 5% even with  $\Delta x = 40$  and  $\Delta t = 20$ .  $E_l$  reduces for smaller  $\Delta t$  and  $\Delta x$ . With  $\Delta x = 10$  and  $\Delta t = 8$ ,  $E_l$  drops to approximately 2.6%. The SMD results obtained by using  $\Delta x = 2$  and  $\Delta t = 1$  is graphically indistinguishable from the MD results obtained by using  $\Delta t = 0.5$ . On the other hand, MD yields erroneous results when  $\Delta t = \Delta t_{cr} = 1$ . Our computation also shows that the energy loss is more sensitive to grid size  $\Delta x$  than to the time step  $\Delta t$ .

Figs. 6 and 7 plot the time-history of the velocity and displacement of the leftmost and middle atoms in the left atom chain, respectively. It can be seen that the high-frequency ripples in the MD results cannot be seen in the SMD results. More

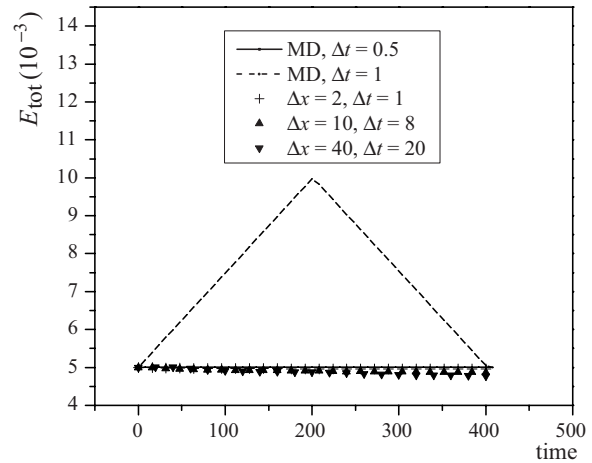


Figure 5: The variation of total energy. Even with  $\Delta x = 40$  and  $\Delta t = 20$ , the energy loss  $E_l < 5\%$ .  $E_l$  will reduce to about 2.6% when  $\Delta t$  decreases to 8

high-frequency ripples can be filtered off by using a larger grid size which in turn enables a larger critical time step.

## 5.2 Tension of a 1D Atom Chain

In this example, an atom chain with 201 atoms uniformly distributed from  $x = 0$  to  $x = 200$  is considered. Initial displacements and velocities of all atoms are zero. Starting from time zero, an external force of magnitude 0.01 along the positive  $x$ -direction is applied to the ten rightmost atoms. All MD results are obtained by using  $\Delta t = 0.5$ . The results are compared with the SMD results with  $(\Delta x, \Delta t)$  taken to be (4, 2), (6, 5) and (11, 10) in Figs. 8 to 11. Fig. 8 shows the computed potential energies. They are almost identical after  $t = 40$  even when the SMD time step is taken to be 10 which is 20 times of the MD time step. Fig. 9 shows the displacements along the atom chain at  $t = 60$  and  $t = 90$  at which the disturbance has not reached the left end of the chain. Excellent agreements are also seen between the MD and SMD results.

Figs. 10 and 11 show the time-history of the velocities and displacements of the two atoms with initial positions  $x = 169$  and  $x = 199$ , respectively. As expected, the velocities yielded by the SMD are significantly smoothed. The displacements yielded by both SMD simulations agree

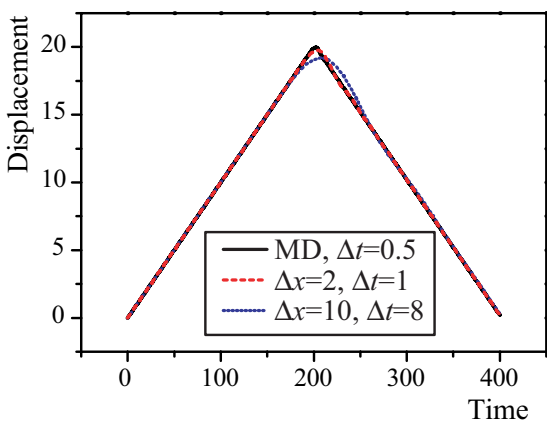
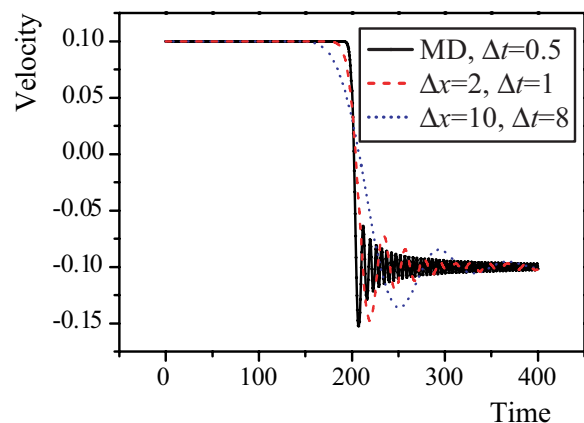


Figure 6: Time history of velocity and displacement of the leftmost atom in the left atom chain

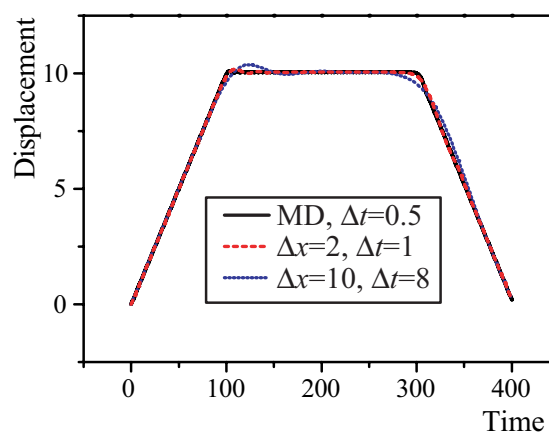
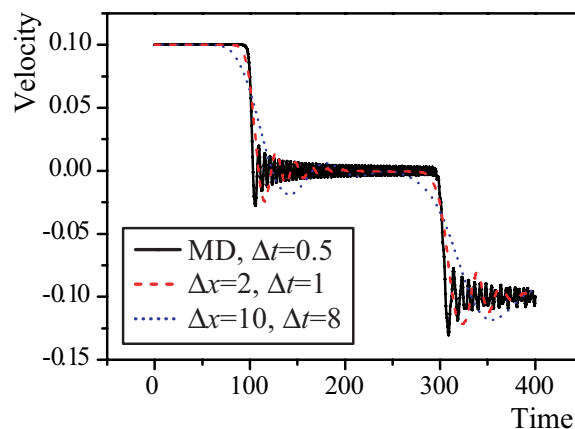


Figure 7: Time history of velocity and displacement of the middle atom in the left atom chain

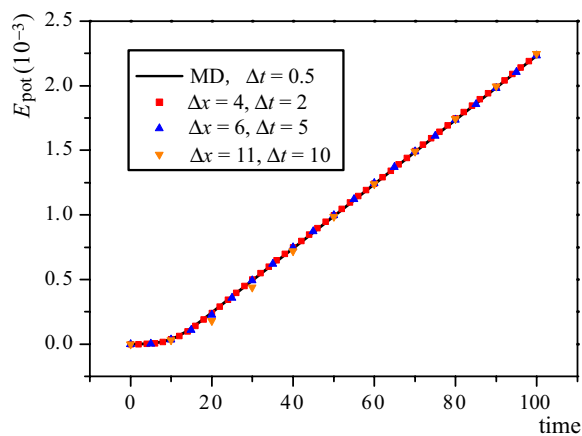


Figure 8: The variation of potential energy versus time

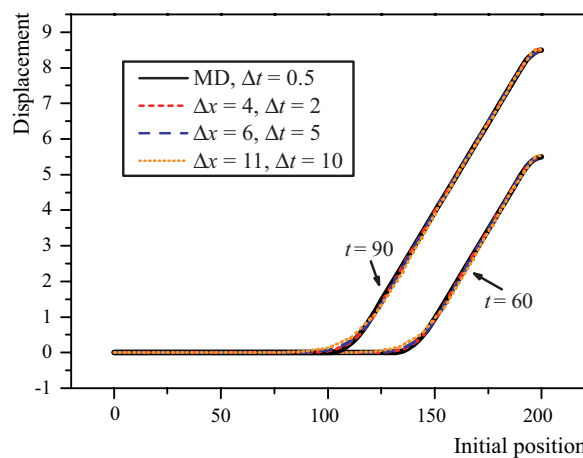


Figure 9: Displacements at the time  $t = 60$  and  $t = 90$

very well with those given by MD. For  $\Delta x = 4$  and  $\Delta t = 2$ , the differences in the displacements between SMD and MD at  $t = 100$  are only 0.22% for the atom initially at  $x = 169$  and 0.03% for the atom initially at  $x = 199$ .

The results of an additional simulation with  $\Delta x = 21$  and  $\Delta t = 20$  are plotted in Fig. 11. In this case, only 5 time steps are used to simulate the whole process of from  $t = 0$  to  $t = 100$ . The time step, which is 40 times of the MD time step, is too large to obtain the velocities at reasonable accuracy. However, the time integration is still stable and the displacements are in good agreement with the MD results.

### 5.3 1D examples with different fundamental frequencies

In the above examples, the potential coefficients of different atom pairs are all the same. Some atom pairs are set to be stiffer in this example to examine the performance of SMD in the problem with different fundamental frequencies.

Similar to the last example, 201 atoms are pulled at the right end. The only difference is that the potential coefficient is set to be  $k_2 = 10$  (ten times the coefficient of the other atom pairs) for the 21th to the 40th atom pairs counted from the right end. According to our computation, the critical time step of MD is about 0.31, which is much lower than that of the last example due to stiffer potentials. Time step  $\Delta t = 0.3$  is used in MD computation. SMD methods with  $(\Delta x, \Delta t)$  equaling (2, 0.6), (4, 1.2) and (10, 3.0) are computed. Results show that good performances can be obtained even in problems with different fundamental frequencies. Fig. 12 and 13 shows the time history of potential energy and displacements along the atom chain. Consistent results are obtained by MD and SMD computations.

### 5.4 Tension/Compression of 3D Single Crystals at High Strain Rate

Tension and compression tests at high strain rate are important tests to identify the time-dependent material properties. Owing to the limitation on computing power, the reported strain rate of MD can only be several orders higher than maximum

experimental strain rate  $10^3 \text{s}^{-1}$  [Lu, Li, and Lu (2001)].

A cubic copper specimen with side length  $30a_0$  where  $a_0 = 3.615 \text{\AA}$  is the lattice constant is isolated from a much larger single-crystal copper. The total number of atoms in the specimen is 108,000. The three coordinate axes are along the [100]-, [010]- and [001]-directions. Periodic boundary conditions are prescribed in all the three directions. The specimen is first relaxed for 10 ps to assume its equilibrium state and then stretched to 5% logarithmic strain. During the loading process, the simulation box is lengthened by 0.001 times along the [001] direction in every picosecond. The other two directions are shortened accordingly to keep the total volume of the specimen unchanged. The system temperature is kept constant at 1 K using the velocity-rescaling technique and Lennard-Jones potential [Agrawal, Rice, and Thompson (2002)] is used in the computation.

Owing to the periodic boundary conditions, the specimen remains to be a rectangular prism. The regular background grid is changed after each time step such that it overlaps with the deformed specimen at the beginning of all time steps. Two SMD simulations are conducted. In the first simulation, the specimen is divided into  $3 \times 3 \times 3$  grid and the time step is taken to be 100 fs which is slightly less than the critical time step ( $\approx 110$  fs). In the second simulation, only one grid cell is used and the time step is taken to be 200 fs which is again slightly less than the critical time step ( $= 210$  fs). On the other hand, the critical time step is 25 fs for the MD. Fig. 14 shows the energy-strain and stress-strain relations. It can be seen that the computed MD and SMD results are graphically indistinguishable. Another cubic specimen with 80,000 atoms compressed to around 10% logarithmic strain is also considered. Again, the computed MD and SMD results can hardly be distinguished.

Table 1 lists the normalized CPU times consumed in the MD and SMD simulations. The computational cost of SMD is around 20% higher than that of MD per time step. However, the present SMD time step sizes are one order larger than the MD

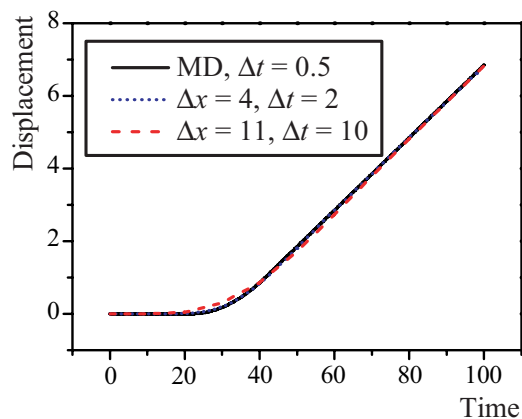
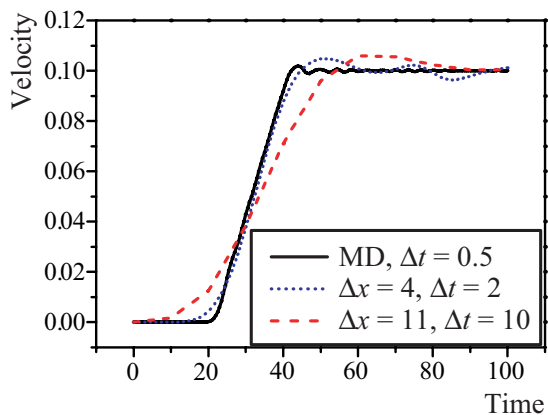


Figure 10: Time-history of velocity and displacement of the atom initially at  $x = 169$ .

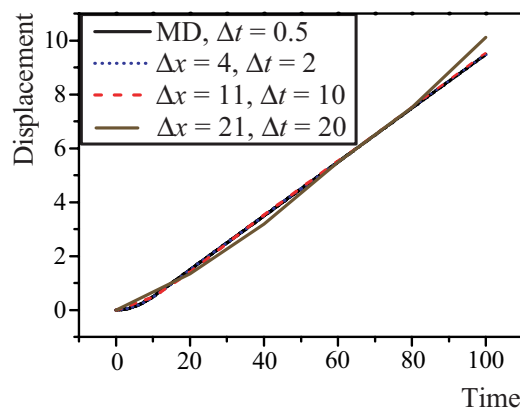
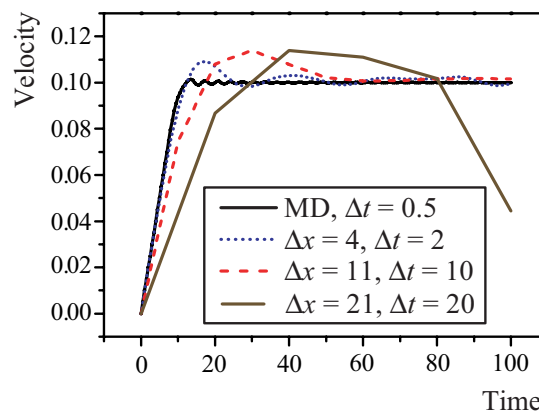


Figure 11: Time-history of velocity and displacement of the atom initially at  $x = 199$ .

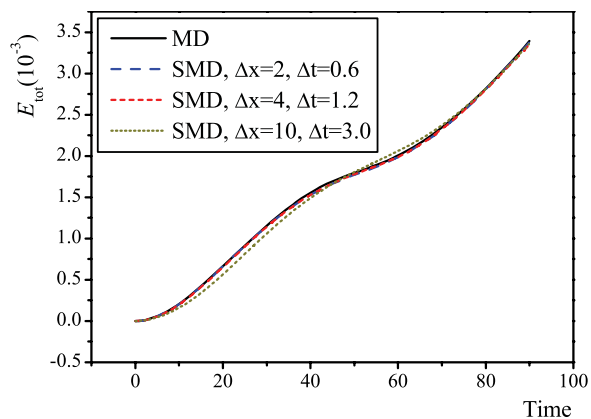


Figure 12: The variation of total energy versus time

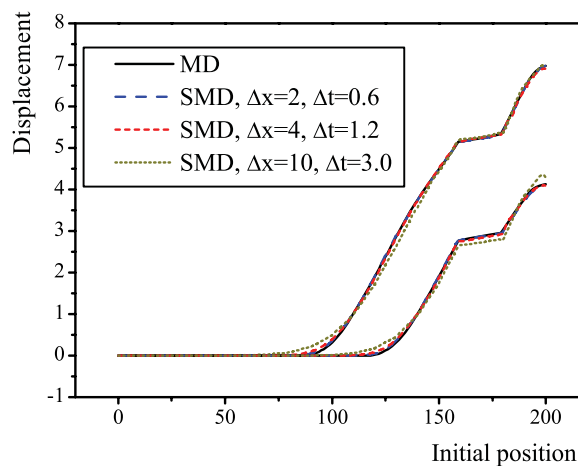


Figure 13: Displacements at the time  $t = 60$  and  $t = 90$

critical time step. Consequently, the SMD CPU times are one order smaller than the MD CPU times.

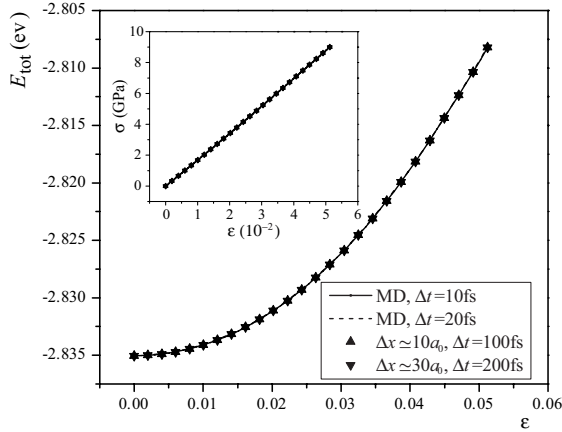


Figure 14: The variation of total energy (outer box) and the stress-strain curve (inner box) for uniform tension of single crystal with periodic conditions. All results are indistinguishable even when the SMD  $\Delta t$  is one order larger than the MD  $\Delta t$ .

Table 1: Normalized CPU times consumed in the MD and SMD simulations. (Simulation details: AMD Athlon 64 Processor 3200+, 2GB memory.)

Method	MD	SMD	SMD	SMD
$\Delta t$ (fs)	10	100	167	200
Tension	1.0	0.124	—	0.065
Compression	1.0	0.123	0.073	—

### 5.5 Tension of a Single Crystal with Free Surfaces

This example considered a cubic specimen within a much larger single-crystal copper and periodic boundary conditions are prescribed over all the specimen surfaces. In this example, a single-crystal copper specimen with free surfaces is considered. Lack of neighboring atoms will increase the potential energy of atoms near the free surfaces so that the distribution of potential energy is not uniform. This example aims to examine the ability of SMD in dealing with non-uniform

deformation. The specimen length is  $10a_0$  in the [001]-direction and,  $20a_0$  in both the [100]- and [010]-directions. The total number of atoms is 16,000. Embedded atom (EAM) potential with the analytical form proposed by Johnson [Johnson (1988)] is adopted here. Periodic boundary condition is prescribed in [001]-direction while the surfaces normal to the [100]- and [010]-directions are left free.

In the simulation, the specimen is first relaxed for 1 ns and then stretched to 8% logarithm strain in the [001]-direction and the strain rate is  $10^8 \text{ s}^{-1}$ . A  $3 \times 3 \times 1$  background grid is used in the SMD computation. Fig. 15 plots the potential energy versus strain relations yielded by MD with  $\Delta t = 10 \text{ fs}$  and SMD with  $\Delta t = 100 \text{ fs}$ . Similar to the previous example, the two set of results are essentially overlapping.

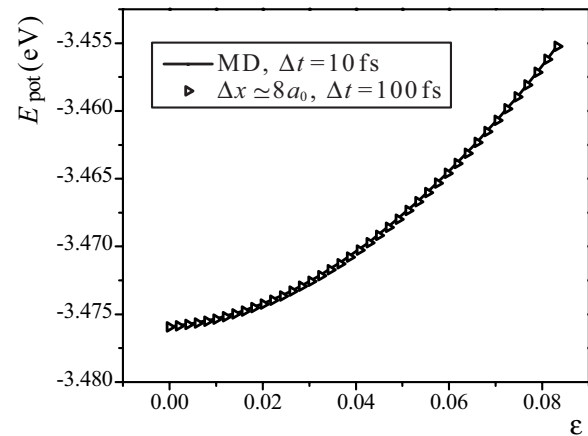


Figure 15: The variation of potential energy versus strain for single crystal specimen with free surfaces under tension

### 5.6 Tension of cracked single crystal

As an example to verify the coupling method, a cracked cuboid specimen shown in Fig. 16 is considered. This specimen is made from perfect single crystal of copper where the atoms in the range  $0 < x < 1.0 \text{ nm}$ ,  $10.75 \text{ nm} < z < 11.25 \text{ nm}$  are removed. The three edges of the specimen are along [100](x), [010](y) and [001](z) directions. The lengths of three edges are 5nm, 5nm and 20nm, respectively. The atoms in the outmost six layers

near the two surfaces perpendicular to the  $z$  axis are moved in a given manner. All the other surfaces are set free. The specimen is first relaxed for 1ns, then the two ends along  $z$  axis are pulled with constant velocity. Constant temperature of 10K are kept in the simulation, and EAM potential is adopted. The tension rate is  $5 \times 10^8 \text{s}^{-1}$ .

MD-SMD coupling method and MD method are used to compute this example. Time step  $\Delta t = 10\text{fs}$  in both the pure MD method and the MD region of the coupling method. A larger time step  $\Delta t = 100\text{fs}$  is used in the SMD region of the coupling method. MD region occupies the central 6nm zone along  $z$  axis, while the other regions are set as SMD region. The background grid covers the whole region to be reached, and the grid cell size is about 2.3nm. The stress-strain curve is shown in Fig. 17. The results of MD method and coupling method matches well. The yield point indicating the startup of plastic mechanism is captured precisely by the coupling method, which shows the good capability of the coupling method to deal with the local disorder.

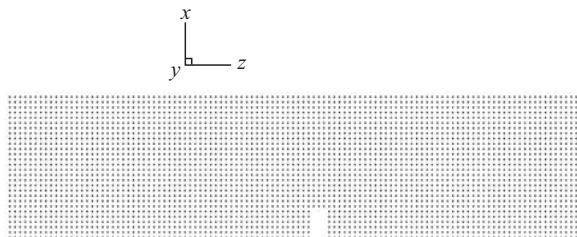


Figure 16: A cracked specimen

## 6 Concluding Remarks

In this paper, a smoothed molecular dynamics (SMD) approach is proposed to enlarge the critical time step in molecular simulations. In SMD, a regular background grid is set up at the beginning of each time step. With the unknowns of the atoms obtained from that of the grid points by interpolation, the unknowns to be solved are reduced from that of the atoms in conventional molecular dynamics (MD) to that of the grid points in the present SMD. To avoid cumulative entanglement and distortion of the grid, the de-

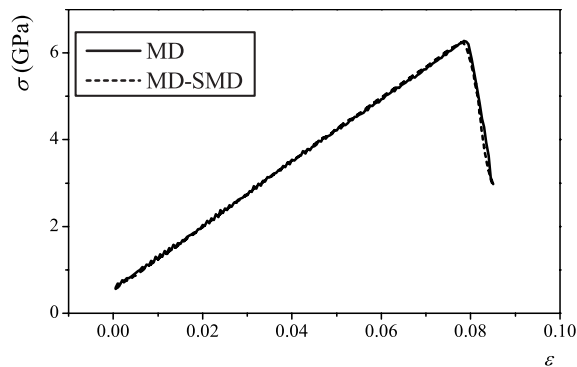


Figure 17: The stress-strain curve of MD and coupled MD-SMD methods

formed grid is discarded at the end of each time step. Besides the mapping process between the atoms and the grid points, the implementation of SMD is very similar to the conventional MD. Any time integration scheme and inter-atomic potential used in the conventional MD can equally be adopted in SMD. The critical time step is controlled by the grid size in SMD instead of the inter-atomic distance in the conventional MD. Consequently, the critical time step can be increased significantly by enlarging the background grid size. Numerical examples show that SMD can yield almost identical results to MD results at much larger time step size.

Coupling of MD and SMD method is briefly discussed in this paper. The coupling process is simple and convenient owing to the similarity of MD and SMD methods. Numerical example shows that coupling method can effectively captures the atom disorder. It may be desired to adopt an adaptive method to partition the problem to different regions. The coupling work is still under development in our group.

**Acknowledgement:** This work was supported by the National Science Foundation of China under grant 10672088, the National Basic Research Program of China under grant 2004CB619304, the Program for New Century Excellent Talents in Universities and the University of Hong Kong.

## References

- Agrawal, P. M.; Rice, B. M.; Thompson, D. L.** (2002): Predicting trends in rate parameters for self-diffusion on fcc metal surfaces. *Surf. Sci.*, vol. 515, pp. 21–35.
- Allen, M. P.; Tildesley, D. J.** (1989): *Computer Simulation of Liquids*. Oxford University Press.
- Andersen, H. C.** (1983): Rattle: A ‘velocity’ version of the shake algorithm for molecular dynamics calculations. *J. Comput. Phys.*, vol. 52, pp. 24–34.
- Ascher, U.; Reich, S.** (1998): On some difficulties in integrating highly oscillatory hamiltonian systems. *Lecture Notes in Computational Science and Engineering*, vol. 4, pp. 281–296.
- Ascher, U.; Reich, S.** (2000): The midpoint scheme and variants for hamiltonian systems: Advantages and pitfalls. *SIAM Journal on Scientific Computing*, vol. 21, pp. 1045–1065.
- Bardenhagen, S. G.; Kober, E. M.** (2004): The generalized interpolation material point method. *CMES: Computer Modeling in Engineering & Sciences*, vol. 5, pp. 477–495.
- Belytschko, T.; Lu, Y. Y.** (1993): Explicit multi-time step integration for first and second order finite element semidiscretizations. *Comput. Meth. Appl. Mech. Eng.*, vol. 108, pp. 353–383.
- Broughton, J. Q.; Abraham, F. F.; Bernstein, N.; Kaxiras, E.** (1999): Concurrent coupling of length scales: Methodology and application. *Phys. Rev. B*, vol. 60, pp. 2391–2403.
- Chun, H. M.; Padilla, C. E.; Chin, D. N.; M, W.; Karlov, V. I.; Alper, H. E.; Soosaar, K.; Blair, K. B.; Becker, O. M.; Caves, L. S. D.; Nagle, R.; Haney, D. N.; Farmer, B. L.** (2000): Mbo(n)d: A multibody method for long-time molecular dynamics simulations. *J. Comput. Chem.*, vol. 21, pp. 159–184.
- Dey, B. K.; Rabitz, H.; Askar, A.** (2003): Optimal reduced dimensional representation of classical molecular dynamics. *J. Chem. Phys.*, vol. 119, pp. 5379–5388.
- Gibson, D. A.; Carter, E. A.** (1993): Time-reversible multiple time scale ab initio molecular dynamics. *J. Phys. Chem.*, vol. 97, pp. 13429–13434.
- Grubmuller, H.; Heller, H.; Windemuth, A.; et al** (1991): Generalized verlet algorithm for efficient molecular dynamics simulations with long-range interactions. *Molecular Simulations*, vol. 6, pp. 121–142.
- Hairer, E.; Wanner, G.** (1991): *Solving Ordinary Differential Equations II: Stiff and Differential-Algebraic Problems*. Springer-Verlag.
- Humphreys, D. D.; Friesner, R. A.; Berne, B. J.** (1994): A multiple-time-step molecular dynamics algorithm for macromolecules. *J. Phys. Chem.*, vol. 98, pp. 6885–6892.
- Izaguirre, J. A.; Catarello, D. P.; Wozniak, J. M.; Skeel, R. D.** (2001): Langevin stabilization of molecular dynamics. *J. Chem. Phys.*, vol. 114, pp. 2090–2098.
- Izaguirre, J. A.; Ma, Q.; Matthey, T.; Willcock, J.; Slabach, T.; Moore, B.; Viamontes, G.** (2002): Overcoming instabilities in verlet-i/r-respa with the mollified impulse method. *Lecture Notes in Computational Science and Engineering*, vol. 24, pp. 146–174.
- Izaguirre, J. A.; Reich, S.; Skeel, R. D.** (1999): Longer time steps for molecular dynamics. *J. Chem. Phys.*, vol. 110, pp. 9853–9864.
- Johnson, R. A.** (1988): Analytical nearest-neighbor model for fcc metals. *Phys. Rev. B*, vol. 37, pp. 3924–3931.
- Leimkuhler, B.; Reich, S.** (1994): Symplectic integration of constrained hamiltonian systems. *Math. Comp.*, vol. 63, pp. 589–605.
- Li, X.; Yang, W.** (2005): Multiple time step molecular dynamics simulation for interaction between dislocations and grain boundaries. *Acta Mechanica Sinica*, vol. 21, pp. 371–379.

- Lu, H.; Daphalapurkar, N. P.; Wang, B.; Roy, S.; Komanduri, R.** (2006): Multiscale simulation from atomistic to continuum — coupling molecular dynamics (md) with the material point method (mpm). *Philos. Mag.*, vol. 86, pp. 2971–2994.
- Lu, L.; Li, S. X.; Lu, K.** (2001): An abnormal strain rate effect on tensile behavior in nanocrystalline copper. *Scripta Materialia*, vol. 45, pp. 1163–1169.
- Ma, Q.; Izaguirre, J. A.; Skeel, R. D.** (2003): Verlet-i/r-respa/impulse is limited by nonlinear instabilities. *SIAM J. Sci. Comput.*, vol. 24, pp. 1951–1973.
- Reich, S.** (1995): Smoothed dynamics of highly oscillatory hamiltonian systems. *Physica D*, vol. 89, pp. 28–42.
- Reich, S.** (1996): Enhanced energy conserving method. *BIT*, vol. 36, pp. 122–134.
- Reich, S.** (1999): Multiple time scales in classical and quantum-classical molecular dynamics. *J. Comput. Phys.*, vol. 151, pp. 49–73.
- Ryckaert, J. P.; Ciccotti, G.; Berendsen, H. J. C.** (1977): Numerical integration of the cartesian equations of motion of a system with constraints: Molecular dynamics of n-alkanes. *J. Comput. Phys.*, vol. 23, pp. 327–341.
- Schlick, T.; Mandziuk, M.; Skeel, R. D.; Srinivas, K.** (1998): Nonlinear resonance artifacts in molecular dynamics simulations. *J. Comput. Phys.*, vol. 140, pp. 1–29.
- Schlick, T.; Skeel, R. D.; Brunger, A. T.; Kale, L. V.; Board Jr., J. A.; Hermans, J.; Schulten, K.** (1999): Algorithmic challenges in computational molecular biophysics. *J. Comput. Phys.*, vol. 151, pp. 9–48.
- Shen, S.; Atluri, S. N.** (2004): Multiscale simulation based on the meshless local petrov-galerkin (mlpg) method. *CMES: Computer Modeling in Engineering & Sciences*, vol. 5, pp. 235–255.
- Shen, S.; Atluri, S. N.** (2005): A tangent stiffness mlpg method for atom/continuum multiscale simulation. *CMES: Computer Modeling in Engineering & Sciences*, vol. 7, pp. 49–67.
- Sulsky, D.; Chen, Z.; Schreyer, H. L.** (1994): A particle method for history-dependent materials. *Comput. Meth. Appl. Mech. Eng.*, vol. 118, pp. 179–196.
- Tan, H. L.; Yang, W.** (1994): Atomistic/continuum simulation of interfacial fracture, part ii: Atomistic /dislocation/continuum simulation. *Acta Mechanica Sinica*, vol. 10, pp. 237–249.
- Tuckerman, M.; Berne, B. J.; Martyna, G. J.** (1992): Reversible multiple time scale molecular dynamics. *J. Chem. Phys.*, vol. 97, pp. 1990–2201.
- Verlet, L.** (1967): Computer ‘experiments’ on classical fluids. i. thermodynamical properties of lennard-jones molecules. *Phys. Rev.*, vol. 159, pp. 98–103.
- Wagner, G. J.; Liu, W. K.** (2003): Coupling of atomistic and continuum simulation using a bridging scale decomposition. *J. Comput. Phys.*, vol. 190, pp. 249–274.
- Zhang, G.; Schlick, T.** (1993): Lin: A new algorithm to simulate the dynamics of biomolecules by combining implicit-integration and normal model techniques. *J. Comput. Chem.*, vol. 14, pp. 1212–1233.
- Zhang, G.; Schlick, T.** (1994): The langevin/implicit-euler/normal-mode scheme for molecular dynamics at large time steps. *J. Chem. Phys.*, vol. 101, pp. 4995–5013.
- Zhang, X.; Sze, K. Y.; Ma, S.** (2006): An explicit material point finite element method for hyper velocity impact. *Int. J. Numer. Meth. Engrg.*, vol. 66, pp. 689–706.
- Zhou, R.; Harder, E.; Xu, H.; Berne, B. J.** (2001): Efficient multiple time step method for use with ewald and particle mesh ewald for large biomolecular systems. *J. Chem. Phys.*, vol. 115, pp. 2348–2358.

